JOURNAL OF CATALYSIS 151, 279–284 (1995)

Cooperative Action of Palladium and Manganese(III) Oxide in the Oxidation of Carbon Monoxide

S. Imamura,*,[1] Y. Tsuji,* Y. Miyake,* and T. Ito†

*Department of Chemistry, Kyoto Institute of Technology, Matsugasaki, Sakyo-Ku, Kyoto 606, Japan; and †School of Social Information Studies, Otsuma Women's University, Karakida, Tama, Tokyo 206, Japan

Received February 9, 1994; revised August 24, 1994

Palladium (Pd) and manganese(III) oxide (Mn_2O_3) cooperated in the oxidation of CO to exhibit high catalytic activity; vapor-phase oxygen was incorporated mainly through Mn_2O_3, and Pd withdrew the oxygen from Mn_2O_3. IR analysis showed that CO was predominantly adsorbed on Pd and that the CO adsorbed on the oxidized state of Pd (Pd^{n+}–CO) was an important intermediate. The CO_2 formed by the oxidation of CO was found to be present on Mn_2O_3 in the form of CO_3. The rate of CO oxidation showed about first-order dependence on CO partial pressure and was independent of the oxygen concentration. Incorporation and activation of vapor-phase oxygen were not rate limiting due to the high affinity of Mn toward oxygen. A reaction path was proposed in which CO was first adsorbed on the oxidized state of Pd, followed by oxidation to form CO_2. The CO_2 migrated to the surface of Mn_2O_3 and was desorbed into the vapor phase. Thus the combination of the oxygen-providing ability of Mn_2O_3 and the inherent high activity of Pd resulted in the improved performance of this composite catalyst.

INTRODUCTION

Oxidation of carbon monoxide has been carried out on various catalysts. These catalysts are precious metals (1–3), perovskite-type catalysts (4–6), transition metal oxide catalysts (7–9), and so on. The activity of the catalysts is sometimes improved remarkably by combining more than two elements (synergism). A famous example of synergism is shown by a gold–iron oxides composite catalyst developed by Haruta *et al.* (10). This catalyst can oxidize carbon monoxide completely at a temperature as low as −70°C. Gold supported on other oxides is also active (11). The synergism in these catalysts is thought to be caused by the interaction of gold and metal oxides at their interface. We also reported previously that manganese–silver composite oxide has high activity in the oxidation of carbon monoxide (12). Its high activity is caused by the difference in their affinities toward oxygen. Manganese adsorbs vapor-phase oxygen easily, while it releases the oxygen rather slowly. On the other hand, oxygen desorption proceeds more easily than its adsorption on silver. Thus manganese adsorbs and activates vapor-phase oxygen and transfers it to silver, which, in turn, donates it to carbon monoxide. In this way, the defects of each element in each rate-limiting step are eliminated. Therefore the combination of different catalyst elements is interesting in oxidation reactions concerning the modification of oxygen mobility on them.

Precious metals are highly active in combustion reactions. Unlike silver, they have moderate oxygen affinity, and, therefore, both activation of vapor-phase oxygen and its release proceed smoothly (13). However, the activity of precious metals may be further increased by combining with other elements which modify the mobility of oxygen. In this work we investigated the synergism of palladium and manganese oxide in the oxidation of carbon monoxide.

EXPERIMENTAL

Catalyst Preparation

1 *N* NaOH was added to an aqueous solution of the nitrate of manganese, cobalt, or iron until the pH of the solution was about 10. The resultant precipitate was washed with deionized water three times, followed by drying at 80°C for 48 h. This dried precipitate (partially dehydroxylated hydroxide) was dispersed in deionized water containing $PdCl_2$ (8 mM) and was stirred for 2 h, followed by evaporation with an evaporator. The amount of $PdCl_2$ used was 0.5 wt% (as metal Pd) of the dried precipitate. This Pd-containing solid was dried at 80°C overnight. Then it was dispersed in deionized water with stirring for 30 min and was filtered; this washing procedure was repeated three times. After the solid was dried at 80°C overnight, it was reduced with hydrogen at 300°C for 2 h, followed by calcination at 300°C in air for 2 h. Pd supported on commercial γ-Al_2O_3 (Nakarai Chemical

[1] To whom correspondence should be addressed.

0021-9517/95 $6.00

Co., BET surface area of 138.5 m^2/g) was prepared by the same procedure as above. Although the valence of Mn in Pd-supported manganese oxide was 2.38, its configuration was determined by X-ray diffraction analysis to be Mn_2O_3; thus this catalyst was denoted as Pd/Mn_2O_3. Pd supported on cobalt oxide, iron oxide, and γ-alumina were also denoted as Pd/Co_3O_4, Pd/Fe_2O_3, and Pd/γ-Al_2O_3, respectively. Manganese(III) oxide without Pd was prepared according to the same procedure except that Pd was not supported. The valence of Mn in it was 2.92 and it was denoted as Mn_2O_3. The BET surface area and the amount of Pd loading were 18.0 m^2/g and 0.19 wt% for Pd/Mn_2O_3, 20.6 m^2/g and 0.36 wt% for Pd/Fe_2O_3, 33.9 m^2/g and 0.41 wt% for Pd/Co_3O_4, and 126.3 m^2/g and 0.27 wt% for Pd/γ-Al_2O_3. The surface area of Mn_2O_3 was 29.2 m^2/g. The catalysts were cut into about 8–14 mesh size before use.

Apparatus and Procedure

Reactions were carried out with an ordinary flow reactor made of quartz (inner diameter of 6 mm) under atmospheric pressure. One ml of the catalysts was used, and the reaction gas (CO, 1%; He, 9%; air, 90%) was passed over the catalysts at a space velocity of 10,000 h^{-1}. The reactions were not affected by any mass transfer limitation because the conversion of CO was independent of the catalyst particle size.

The weight change of the catalysts in the oxidation-reduction experiment was monitored with a Rigaku Denki CN8068 A1 thermobalance under a flow of oxygen or hydrogen.

Temperature programmed desorption (TPD) of oxygen from the catalysts was carried out with a quartz vessel connected to an ordinary vacuum line and a Ulvac MSQ-150 quadrupole mass spectrometer. The temperature of the vessel was increased at a rate of 10°C/min under vacuum.

Analyses

The reacted gas was introduced into the column (activated charcoal 1 m plus molecular sieve 5A 1 m) of a Shimadzu GC-8A gas chromatograph at 120°C to separate CO and CO_2. Then they were converted into methane by using a Shimadzu MNT-1 methanizer attached inside the gas chromatograph and were analyzed by a FID detector.

The average valence of Mn in the catalyst was determined colorimetrically by dissolving the catalyst in a 1 *N* sulfuric acid solution of Mohr's salt. The details of this procedure are described elsewhere (12).

IR spectra were obtained with a Nihon Denshi JIR-6500W FTIR spectrophotometer with a diffuse reflectance attachment.

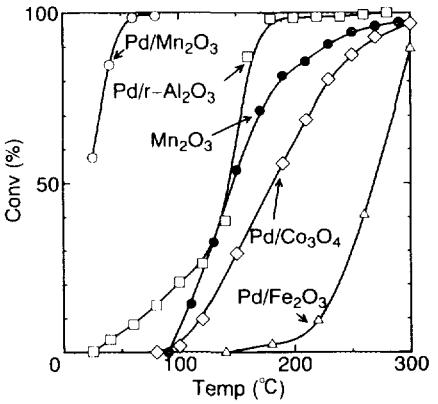

FIG. 1. Oxidation of CO. [CO] = 1%, catalyst = 1 ml, space velocity = 10,000 h^{-1}. The temperature of the catalyst bed was increased at a rate of 3.75°C/min.

RESULTS AND DISCUSSION

Effect of the Kind of Metal Oxides on the Activity of Pd

Figure 1 shows the change in CO conversion with increasing reaction temperature; the temperature of the catalyst bed was increased at a rate of 3.75°C/min. Pd/Mn_2O_3 exhibited the highest activity. As the activities of Mn_2O_3 and Pd/γ-Al_2O_3 were much lower than that of Pd/Mn_2O_3, synergism of Pd and manganese appeared. The activities of Pd/Fe_2O_3 and Pd/Co_3O_4 were low. From the data shown in Fig. 1, specific rate of the reaction (moles of CO converted per unit surface area of the catalyst per unit reaction time) was plotted against reaction temperature (Fig. 2). Figure 2 also shows that Pd/Mn_2O_3 is remarkably active compared with other catalysts. As the true active sites of the catalysts are not known, however, this analysis may not reflect the true activity order of these catalysts;

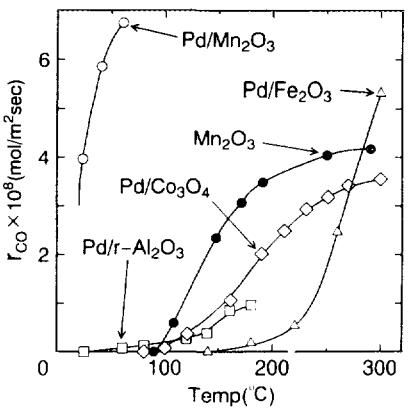

FIG. 2. Specific rate of CO conversion (r_{co}) vs reaction temperature. The reaction condition is shown in Fig. 1.

for example, alumina surfaces which are not covered with Pd do not seem to act as active sites. However, when the rate of the oxidation of CO per unit amount of Pd was plotted against reaction temperature, the same result as shown in Figs. 1 and 2 was obtained; that is, Pd/Mn_2O_3 was the most active.

In a separate experiment, Pd-supported catalysts (Pd/Mn_2O_3, Pd/Co_3O_4, and Pd/Fe_2O_3) were prepared by a different method as follows. After impregnation of $PdCl_2$ on dried hydroxides of Co, Mn, and Fe (0.5 wt% as metal Pd) by using an evaporator, the catalysts were again dispersed in deionized water and pH was adjusted to 11. An excess amount of HCHO over Pd (fivefold moles) was added, and the solution was heated at 80°C for 30 min with stirring. Then the catalysts were filtered, washed three times with deionized water, dried at 80°C overnight, and finally calcined at 300°C for 2 h in air. The temperatures at which complete oxidation of CO occurred on these catalysts were 100°C for Pd/Co_3O_4 and Pd/Mn_2O_3, and 125°C for Pd/Fe_2O_3. Thus the activity of the catalysts depends on the method of preparation. Although we also examined other methods; the most active catalyst was found to be Pd/Mn_2O_3 prepared by the procedure described under Experimental. Therefore we used this type of Pd-supported Mn_2O_3 catalyst thereafter.

Although we tried to estimate the particle size of Pd in this catalyst by a TEM technique, no image of Pd was observed; the Pd species seemed to be finely dispersed on the surface of Mn_2O_3. An ESCA analysis did not give enough information on Pd. Therefore, the state of the Pd was left unknown.

Behavior of Pd/Mn_2O_3 in Desorption and Incorporation of Oxygen

Figure 3 shows the oxygen–TPD spectra of Pd/Mn_2O_3 and Mn_2O_3. In this case the catalysts were not reduced by hydrogen previously because reduction in the presence of Pd resulted in the excess reduction of Mn_2O_3 as shown below. Thus the dried hydroxides were pretreated with oxygen at 200°C for 1 h in the vessel of TPD apparatus in order to adjust the valence of Mn in both catalysts (2.82). After evacuation at 0°C for about 5 h, the temperature of the catalyst vessel was increased at a rate of 10°C/min. Pd/Mn_2O_3 desorbed larger amounts of oxygen than Mn_2O_3. Especially oxygen was desorbed from Pd/Mn_2O_3 even in the low temperature region below 200°C where Mn_2O_3 released scarce oxygen. It was found in a separate experiment that PdO released its lattice oxygen at 380°C. However, Pd/Mn_2O_3 desorbed little oxygen in this temperature region. Thus the desorption of the oxygen belonging to the Pd is negligible even if we assume that all the Pd was in the form of PdO; the amount of Pd loaded on Pd/Mn_2O_3 was only 0.19 wt%. These results indicated

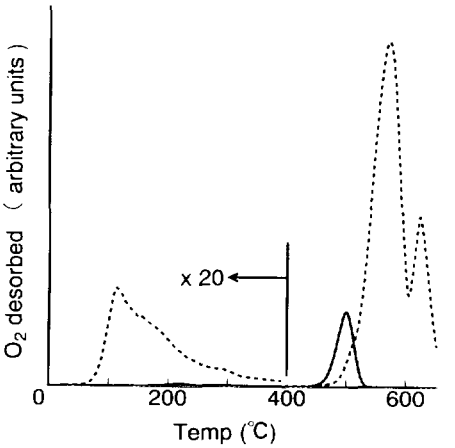

FIG. 3. TPD of oxygen from Mn_2O_3 (—) and Pd/Mn_2O_3 (---). The sensitivity of the detector was magnified by 20 times in the temperature range below 400°C.

that Pd withdrew oxygen belonging to Mn and promoted its desorption. The same phenomenon was observed for manganese–silver composite oxide, in which silver withdrew oxygen from Mn and released it into the vapor phase (12).

In order to further see the effect of Pd on the desorption or incorporation of oxygen from or into Mn_2O_3, the Pd/Mn_2O_3 and Mn_2O_3 prepared in the same manner as in the above experiment were reduced with hydrogen and oxidized with oxygen repeatedly in the chamber of a thermobalance. The extent of oxidation and of reduction was expressed by the change in x of MnO_x calculated from the weight change of the catalysts (Table 1). The starting value of x was 1.41 as shown above. Oxidation and reduction were carried out until no further weight change occurred (usually within 5 min); nitrogen was introduced between the oxidation and reduction procedures. Much more oxygen was removed by hydrogen from Pd/Mn_2O_3 ($x = 1.00$) than from Mn_2O_3 ($x = 1.38$) at 200°C. This may again show the effect of Pd to withdraw oxygen, although the reduction may have occurred on the surface of Mn_2O_3 by the hydrogen spilled over from Pd to Mn_2O_3. When oxygen was introduced instead, reoxidation of Mn in Pd/Mn_2O_3 did not occur at 200°C. After further reduction at 300°C, Pd/Mn_2O_3 began to absorb oxygen. In the case of Mn_2O_3 reoxidation took place after the reduction at 300°C. The reduction–oxidation behavior of both catalysts suggests that Mn_2O_3 absorbs oxygen more easily than Pd/Mn_2O_3. Even at a deeply reduced state ($x = 1.0$, reduction at 200°C) Pd/Mn_2O_3 did not absorb oxygen at 200°C, whereas Mn_2O_3 absorbed oxygen at a less reduced state ($x = 1.26$, reduction and oxidation at 300°C). Moreover, Mn_2O_3 absorbed much more oxygen than Pd/Mn_2O_3 at the same oxidation temperature of 300°C despite its less reduced state compared with that of Pd/Mn_2O_3 ($x =$

TABLE 1

Oxidation and Reduction of Pd/Mn_2O_3 and Mn_2O_3

Catalyst	Treatment[a] Gas	Temp (°C)	x in MnO_x[b]
Pd/Mn_2O_3	O_2	200	1.41
	H_2	200	1.00
	O_2	200	1.00
	H_2	300	0.82
	O_2	300	1.00
Mn_2O_3	O_2	200	1.41
	H_2	200	1.38
	O_2	200	1.38
	H_2	300	1.26
	O_2	300	1.35
	H_2	400	0.92
	O_2	300	1.22

[a] Oxidation by O_2 and reduction by H_2 (both with a flow rate of 40 ml/min) were carried out until no weight change of the catalysts was observed.

[b] Manganese was supposed to be in the form of MnO_x for convenience. As the valence of Mn in the starting catalysts was 2.84, the initial value of x was assigned as 1.41. The change of x was calculated from weight gain or loss of the catalysts, assuming that the weight change was solely due to the change in the content of oxygen.

0.92 for the former and 0.82 for the latter). These facts indicate that Pd does not promote the incorporation of oxygen into Mn_2O_3. Thus it can be concluded that the Mn, and not the Pd, in this composite catalyst plays the role to incorporate oxygen from the vapor phase.

The kinetics for the oxidation of CO on both catalysts were investigated under the condition of a differential reactor (in the CO conversion range less than 15%). The reactions were carried out at 25°C, and the catalysts were diluted with quartz sand to 2.0 wt% in order to maintain the conversion of CO below 15%. The ranges of the partial pressure of CO and of oxygen examined were 3–38 Torr and 15–190 Torr (1 Torr = 133.3 Pa), respectively. The rate expressions were obtained as follows:

$$r_{CO} = k[CO]^{1} \cdot {}^{2}[O_2]^{0} \cdot {}^{1} \quad \text{for } Pd/Mn_2O_3$$
$$r_{CO} = k'[CO]^{1} \cdot {}^{0}[O_2]^{0} \quad \text{for } Mn_2O_3.$$

The order with respect to oxygen was almost zero for both catalysts, suggesting that the incorporation of oxygen from the vapor phase is not rate limiting.

IR Analyses and the Reaction Path for CO Oxidation over Pd/Mn_2O_3

IR analyses were carried out in order to obtain information on the reaction path. The catalysts were evacuated at 300°C for 1 h before introduction of CO. As shown in Fig. 4A, an introduction of CO over Pd/Mn_2O_3 formed an adsorbed species with an absorption band at 2020 cm^{-1}, which was due to CO linearly bonded to Pd^0 (Pd^0–CO) (14). When CO was introduced on Pd/Mn_2O_3 pre-evacuated at 150°C, absorption bands were observed at 2090 cm^{-1} due also to Pd^0–CO and at 1980 cm^{-1} due to CO species bridged over two Pd atoms (Pd_2 > CO) (15); however, they are not shown in the figure. Although the change in the pretreatment condition resulted in the different catalyst states and, hence, in the differently adsorbed CO species, these results show that CO readily interacts with Pd. A very weak absorption band also appeared at 2175 cm^{-1} (Fig. 4A), which was assumed to be due to CO adsorbed on an oxidized state of Mn (Mn^{n+}–CO) (16). When 80 Torr of oxygen was introduced, the band due to Pd^0–CO disappeared while that of Mn^{n+}–CO remained unchanged (Fig. 4B), and new bands appeared at 2145 cm^{-1} and in the range from 1800 to 1100 cm^{-1}. The band at 2145 cm^{-1} was due to CO adsorbed on oxidized state of Pd (Pd^{n+}–CO) (17). The bands in the region from 1800 to 1100 cm^{-1} were assumed to be due mainly to bidentate carbonate (CO_3) adsorbed on oxidized state of Mn (18, 19), although other carbonate species may have been present. The intensity of the bands of bidentate carbonate tended to increase with time (Figs. 4C and 4D). Evacuation at room temperature for 10 min decreased the intensity of all absorption bands (Fig. 4E).

The result of CO adsorption on Mn_2O_3 is shown in Fig. 5. On an introduction of CO (20 Torr), absorption bands due to Mn^{n+}–CO (2175 cm^{-1}) and bidentate carbonate (1800–1100 cm^{-1}) appeared (Fig. 5A). Although 80 Torr of oxygen was introduced successively, intensity of these band scarcely increased (Figs. 5B and 5C). Moreover the intensity of the bidentate carbonate species was much weaker than that on Pd/Mn_2O_3 (Figs. 4B–4D). This im-

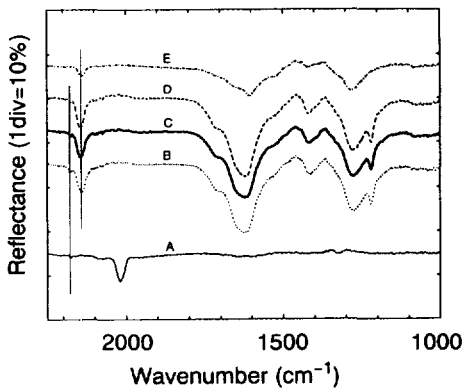

FIG. 4. IR spectra of adsorbed species on Pd/Mn_2O_3. (A) 1 h after an introduction of 20 Torr of CO, (B) 5 min after successive introduction of 80 Torr of O_2, (C) after 30 min, (D) after 1 h, and (E) 10 min after evacuation (from the state of (D)) at room temperature. Pd/Mn_2O_3 was pretreated at 300°C for 1 h under vacuum.

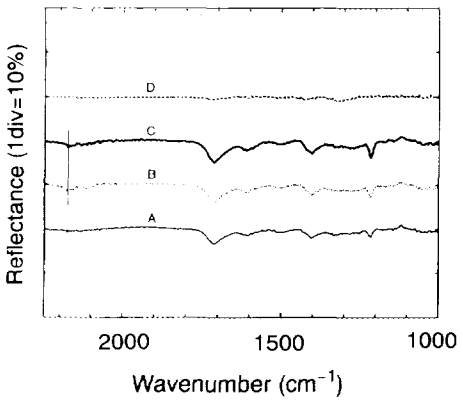

FIG. 5. IR spectra of adsorbed species on Mn_2O_3. (A) 1 h after an introduction of 20 Torr of CO, (B) 5 min after successive introduction of 80 Torr of O_2, (C) after 1 h, and (D) 10 min after evacuation (from the state of C) at room temperature. Mn_2O_3 was pretreated at 300°C for 1 h under vacuum.

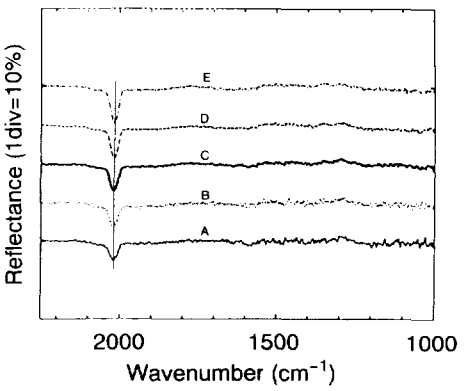

FIG. 6. IR spectra of CO absorbed on Pd/Mn_2O_3 pretreated at 300°C for 1 h under vacuum. (A) 1 min after an introduction of 0.8 Torr of CO, (B) after 3 min, (C) after 10 min, (D) after 30 min, (E) after 1 h.

plies that Mn does not play the main role to oxidize CO and that the active site oxidizing CO is Pd. Evacuation at room temperature resulted in the disappearance of all absorption bands, showing that CO and carbonate species on Mn_2O_3 desorbs quite easily (Fig. 5D).

Pd, not Mn_2O_3, seems to be the site for CO adsorption because only a trace amount of adsorbed CO was present on Mn (the band at 2175 cm^{-1} shown in Figs. 4 and 5) whereas Pd formed various adsorbed CO species. Kinetics indicated that the oxidation of CO on Pd/Mn_2O_3 showed about first-order dependence on CO partial presssure. This probably implies that the adsorption of CO is rather slow and rate determining. It is known that the rate of oxidation of CO on various precious metals is inversely proportional to CO partial pressure (20, 21); CO rapidly covers the surface of precious metals and prevents oxygen from approaching the metal surface. If the present reaction proceeds via the adsorption of CO on the oxidized state of Pd (Pd^{n+}–CO: the absorption band at 2145 cm^{-1} shown in Fig. 4), this step would not be so rapid because palladium oxides cannot have back-donating interaction with CO unlike Pd metal (22, 23). Therefore the first-order dependence of the reaction rate on CO pressure would result. However, the possibility of the role of CO adsorbed on metallic Pd cannot be excluded completely. For example, adsorption of CO on metallic Pd (2020 cm^{-1}) did not proceed so rapidly in the present case; under 0.8 Torr of CO the intensity of this band increased with time rather slowly (Fig. 6). This result may also explain the reaction order of unity with respect to CO pressure. However, as enough oxygen is present under the reaction condition and Pd also withdraws oxygen from Mn_2O_3, it is reasonable to assume that the surface of Pd is covered with oxygen in its working state and CO is adsorbed on the oxidized Pd in the first step of the reaction; that is, Pd^{n+}–CO (2145 cm^{-1}) is the intermediate.

From the results obtained so far, the reaction path was deduced for the oxidation of CO on Pd/Mn_2O_3 (Fig. 7). Pd easily withdraws oxygen from Mn_2O_3 (Fig. 7A) and, thus, the surface of Pd is covered with a thin layer of Pd oxides. The CO is adsorbed on this oxidized Pd (Fig. 7B). The first-order dependence of the rate on CO concentration seems to show that this step proceeds rather slowly. Mn, not Pd, incorporates oxygen from vapor phase (Fig. 7C) and transfers it to Pd (Fig. 7A). This will occur quite easily as a non rate-limiting step because the reaction was not affected by oxygen partial pressure. As Mn has scarce oxidizing ability at room temperature as verified by IR analyses, Pd should oxidize CO. However, the oxidation ability of Pd seems to be enhanced by the combination with Mn_2O_3, considering the low activity of $Pd/\gamma\text{-}Al_2O_3$. The active site may be the interface between Mn_2O_3 and Pd where much active oxygen is provided from Mn assisted by the oxygen-withdrawing ability of Pd. The CO_2 formed at this active site (Fig. 7D) will migrate to the surface of Mn_2O_3 (Fig. 7E) in the form of CO_3 (IR result: Figs. 4B–4D) and is desorbed into the vapor phase (Fig. 7F). This step (Fig. 7F) seems not to be rate limiting

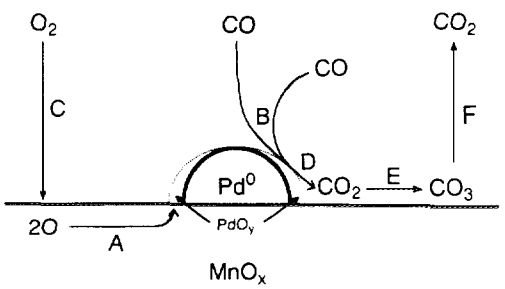

FIG. 7. Supposed reaction path.

because the bidentate carbonate on Mn^{n+} desorbed rather easily on evacuation (Fig. 4E and Fig. 5D).

ACKNOWLEDGMENTS

The authors thank K. Utani of the Kyoto Institute of Technology for his kind cooperation. They also express their gratitude to Dr. Y. Saito of the same Institute for his help in the TEM analysis.

REFERENCES

1. Yao, Y. Y., *Ind. Eng. Chem. Prod. Res. Dev.* **19,** 293 (1980).
2. Kim, Y., Shi, S. K., and White, J. H., *J. Catal.* **61,** 374 (1980).
3. Yao, Y. Y., *J. Catal.* **87,** 152 (1984).
4. Voorhoeve, R. J. H., Remika, J. P., Freeland, P. E., and Matthias, B. T., *Science* **177,** 353 (1972).
5. Voorhoeve, R. J. H., Johnson, D. W., Jr., Remika, J. P., and Gallagher, P. K., *Science* **195,** 827 (1977).
6. Gallagher, P. K., Johnson, D. W., Jr., and Vogel, E. M., *J. Am. Ceram. Soc.* **60,** 28 (1977).
7. Almquist, J. A., and Bray, W. C., *J. Am. Chem. Soc.* **45,** 2305 (1923).
8. Bray, W. C., and Doss, G. J., *J. Am. Chem. Soc.* **48,** 2060 (1926).
9. Severino, F. and Laine, J., *Ind. Eng. Chem. Prod. Res. Dev.* **22,** 396 (1983).
10. Haruta, M., Yamada, N., Kobayashi, T., and Iijima, S., *J. Catal.* **115,** 301 (1989).
11. Haruta, M., Tsubota, S., Ueda, A., and Sakurai, H., *in* "New Aspects of Spillover Effect in Catalysis" (T. Inui, K. Fujimoto, and M. Masai, Eds.), p. 45, *Stud. Surf. Sci. Catal.*, Vol. 77. Elsevier, Amsterdam, 1993.
12. Imamura, S., Sawada, H., Uemura, K., and Ishida, S., *J. Catal.* **109,** 198 (1988).
13. Haruta, M. and Sano, H., *in* "Preparation of Catalysts III" (G. Poncelet, P. Grange, and P. A. Jacob, Eds.), p. 225. Elsevier, Amsterdam, 1983.
14. Guglielminotti, E., and Boccuzzi, F., *in* "Structure and Reactivity of Surfaces" (C. Morterra, A. Zecchina, and G. Costa, Eds.), p. 437. Elsevier, Amsterdam, 1989.
15. Anderson, J. A., and Rochester, C. H., *J. Chem. Soc., Faraday Trans.* **87,** 1479 (1991).
16. Knozinger, H., *in* "Acid Base Catalysis" (K. Tanabe, H. Hattori, T. Yamaguchi, and T. Tanaka, Eds.), p. 147. Kodansha, Tokyo, 1989.
17. Marchese, L., Boccuti, M. R., Coluccia, S., Lavagnino, S., Zecchina, A., Bonneviot, L., and Che, M., *in* "Structure and Reactivity of Surfaces" (C. Morterra, A. Zecchina, and G. Costa, Eds.), p. 653. Elsevier, Amsterdam, 1989.
18. Philipp, R., and Fujimoto, K., *J. Phys. Chem.* **96,** 9035 (1992).
19. Little, L. H. (Ed.), "Infrared Spectra of Adsorbed Species," p. 47. Academic Press, London, 1966.
20. Oh, S. H., and Eickel, C. C., *J. Catal.* **112,** 543 (1988).
21. Yao, Y. Y., *J. Catal.* **87,** 152 (1984).
22. Rasband, P. B., and Hecker, W. C., *J. Catal.* **139,** 551 (1993).
23. Baddour, R. F., Modell, M., and Heusser, U. K., *J. Phys. Chem.* **72,** 3621 (1968).